The top quark right coupling in the tbW-vertex

Gabriel A. González-Sprinberg[*1] and Jordi Vidal[†2]

[1]Instituto de Física, Facultad de Ciencias, Universidad de la República, Iguá 4225, Montevideo 11600, Uruguay.
[2]Departament de Física Teòrica, Universitat de València, and Instituto de Física Corpuscular (IFIC), Centro Mixto Universitat de València-CSIC, E-46100 Burjassot, València, Spain.

December 16, 2015

Abstract

The most general parametrization of the *tbW* vertex includes a right coupling V_R that is zero at tree level in the standard model. This quantity may be measured at the Large Hadron Collider where the physics of the top decay is currently investigated. This coupling is present in new physics models at tree level and/or through radiative corrections, so its measurement can be sensitive to non standard physics. In this paper we compute the leading electroweak and QCD contributions to the top V_R coupling in the standard model. This value is the starting point in order to separate the standard model effects and, then, search for new physics. We also propose observables that can be addressed at the LHC in order to measure this coupling. These observables are defined in such a way that they do not receive tree level contributions from the standard model and are directly proportional to the right coupling. Bounds on new physics models can be obtained through the measurements of these observables.

1 Introduction

Top quark physics is now a high statistics physics, mainly due to the huge amounts of data coming from the Large Hadron Collider (LHC) run I and, now, run II [1, 2]. It is strongly believed that, due to its very high mass, the top quark will be a window to new physics [3]. This can be easily understood in the effective lagrangian approach, where the new physics contributions can be parametrized in a series expansion in terms of the parameter m_t/Λ, where m_t is the top quarks mass and Λ is the new physics scale. Besides, most of the top quark properties and couplings are known with a precision

[*]gabrielg@fisica.edu.uy
[†]vidal@uv.es

arXiv:1510.02153v3 [hep-ph] 15 Dec 2015

far below than the other quarks and than the other standard model (SM) particles. It is the only quark that weakly decays before hadronization but, up to now, only one decay mode, $t \to bW^+$, is known. For instance, many extensions of the SM predict new decay modes that can be accessible at LHC. The top quark was detected for the first time at TEVATRON [4,5], where many of its physical properties where measured and some bound on the anomalous Wtb couplings were set [6–8]. Nowadays, top physics is intensively investigated in theoretical research [3] and at the LHC [1,2,9], as the reader can verified in the ATLAS and CMS web pages. In particular, the measurements of the different helicity components of the W in the top decay allows to study the tbW Lorentz vertex structure [10]. These studies were extended in recent years [11–15]. There, the longitudinal and transverse helicities of the W coming from the top decay were investigated and they show that a precise determination of the Lorentz form factors of the vertex can be done with a suitable choice of observables. The most general parametrization of the on-shell vertex needs four couplings, but in the SM three of them are zero at tree level while only the usual left, coupling V_L is not zero and with a value close to one [16]. This is not the case in extended models where, in addition, some of these couplings can also be sensitive to new CP-violation mechanisms.

The right top coupling is largely unknown and deserves a careful study. The other two couplings, usually called tensorial couplings, were investigated at the LHC [17] and will not be considered here. The predictions for the SM, for the two-Higgs-doublet model (2HDM) and other extended models where recently considered in refs. [18–20]. In this paper we first compute the right coupling V_R in the SM at leading order, and define appropriate observables in order to have direct access to it. The former one loop calculation is needed in order to disentangle SM and new physics effects in the observables. Next, we will introduce a set of observables that allows to perform a precise search of the V_R coupling. We obtain a combination of observables directly proportional to it in such a way that they are not dominated by the leading tree level SM contribution V_L. These observables can be an important tool in order to measure new physics contributions to V_R.

This paper is organized as follows. In the next section we introduce a precise definition of the right coupling and compute the first order QCD and electroweak (EW) contributions. In section 3 we present and discuss a set of observables that can be measured with LHC data, both in the polarization matrix and in the spin correlations. Finally, we discuss the results and present our conclusions in section 4.

2   Right top tbW coupling in the SM

Considering the most general Lorentz structure for on-shell particles, the $\mathcal{M}_{tbW}$ amplitude for the $t(p) \to b(p')W^+(q)$ decay can be written in the following way:

$$
\begin{aligned}
\mathcal{M}_{tbW} \;=\; & -\frac{e}{\sin\theta_w \sqrt{2}} \epsilon^{\mu*} \times \\
& \overline{u}_b(p') \left[\gamma_\mu (V_L P_L + V_R P_R) + \frac{i\sigma_{\mu\nu} q^\nu}{M_W}(g_L P_L + g_R P_R) \right] u_t(p),
\end{aligned} \tag{1}
$$

where the outgoing W^+ momentum, mass and polarization vector are $q = p - p'$, M_W and ϵ^μ, respectively. The form factors V_L and V_R are the left and right couplings, respectively, while g_L and g_R are the so called tensorial or anomalous couplings.

The expression (1) is the most general model independent parametrization for the tbW^+ vertex. Within the SM, the W couples only to left particles then, at tree level, all the couplings are zero except for V_L that is given by the Kobayashi-Maskawa matix element $V_L = V_{tb} \simeq 1$ [16]. At one loop all of these couplings receive contributions from the SM. For example, the real and imaginary parts of the g_L and g_R couplings were calculated in the SM [18] and in a general alligned-2HDM [19].

The one loop electroweak and QCD contributions to the V_R coupling can be calculated just by considering the vertex corrections shown in figure 1 and extracting from them the Lorentz structure corresponding to the V_R coupling. Note that this Lorentz structure is not present in the SM lagrangian so, at one loop, there is no need for any counter-term for this contribution. For this reason, the SM one-loop contribution to the V_R coupling is finite. This is similar to what happens for the top $g_{L,R}$ couplings [18, 19]. We will denote each diagram by the label ABC according with the particles running
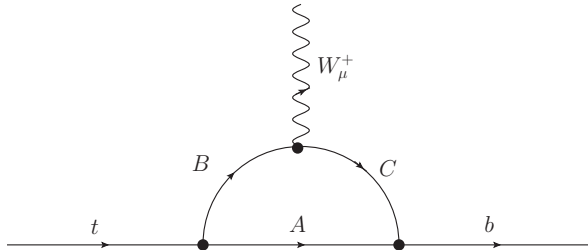

Figure 1: One-loop contributions to the V_R coupling in the $t \to bW^+$ decay.

in the loop. In addition to the usual notation for the SM particles we use the symbols w_0 and w for the neutral and charge would-be Goldstone bosons, respectively, and H for the SM Higgs. There are 18 diagrams that have to be considered and the one loop V_R value one gets from them is finite, without the need of renormalization as already stated. In particular, the one-loop contributions from diagrams tw_0w, tHw, bww_0, bwH, w_0tb and Htb are ultraviolet (UV) divergent. However, when summing them up by pairs (i.e. $tw_0w + tHw$, $bww_0 + bwH$ and $w_0tb + Htb$), the result is finite. The electroweak contributions of all the diagrams are given in the appendix A in terms of parametric integrals. For the UV divergent diagrams we present the sum of the two diagrams that cancels the divergence, as can be seen in eqs. (46), (52) and (57). There, the first (second) term, in each of these expressions, corresponds to the UV safe sector of the first (second) diagram, while the third one corresponds to the sum of the UV divergent part of the two diagrams that results in a finite contribution, as it should be.

All the contributions can be written as:

$$V_R^{ABC} = \alpha \, V_{tb} \, r_b \, I^{ABC}, \tag{2}$$

where $r_b = m_b/m_t$ and I^{ABC} is an integral shown in appendix A for all the diagrams that contribute to V_R. As expected, all the contribution are proportional to the bottom mass through r_b.

3

When one of the particles circulating in the loop is a photon the integral can be performed analytically. Then, the contribution can be written as

$$V_R^{ABC} = \frac{\alpha}{8\pi} V_{tb} \, Q_A \, I_0^{ABC}, \tag{3}$$

with Q_A being the charge of the A-quark circulating in the loop in units of $|e|$ (for the γtb diagram, $Q_A = Q_t \cdot Q_b$). The I_0^{ABC} analytical expressions, as well as their limits for $r_b \to 0$, are shown in appendix B. All these expressions were used as a check of our computations.

The leading QCD contribution can be easily obtained from eq. (56) just by substituting the couplings of the photon by the gluon ones, so we get:

$$V_R^{gtb} = -\frac{\alpha_s}{8\pi} \, C_F \, V_{tb} I_0^{\gamma tb}, \tag{4}$$

with $I^{\gamma tb}$ given in eq. (62) and (67), and $C_F = 4/3$ is the color factor.

With the set of values of ref. [16], the numerical values for the contribution to V_R of each diagram and the complete one-loop SM value are given in table 1, for $V_{tb} = 1$.

In this table the contribution from the UV divergent diagrams are summed up to get a finite result; the first (second) quantity between brackets corresponds to the finite contribution of the first (second) diagram, and the third one (which is logarithmic) is the finite sum of the two UV divergent parts.

As can be seen in table 1, even though the contribution of most of the diagrams is of the order of 10^{-5} for the real part of the V_R coupling, the total EW contribution is, at the end, two orders of magnitude smaller due to the accidental cancellations among the diagrams. The QCD contribution is real and four orders of magnitude bigger than the real EW one so that the real part of the V_R coupling is dominated by the former. The imaginary part, instead, remains of order 10^{-5}, and it is purely EW.

3 Observables

In general, the LHC observables considered in the literature are not very sensitive to the right coupling V_R. This is due to the fact that this coupling comes from a lagrangian term that has the same parity and chirality properties than the leading coupling V_L so that the observables receive contributions from both terms. These observables are the angular asymmetries in the W rest frame [10, 11, 21, 22], angular asymmetries in the top rest frame [11, 22–24] and spin correlations [11, 22, 25, 26]. Our strategy will be to define observables directly proportional to V_R considering the dependencies on the coupling terms. Similar ideas were widely applied when investigating tau physics dipole moments [27, 28]. For top decays, one way to suppress the V_L contribution is to define observables where only right polarized quarks contribute, but this polarization is not accessible to the present facilities and experiments. Given the results shown in the previous section, from now on we always assume that the imaginary part of the V_R coupling is negligible.

Table 1: Contribution to V_R from the different diagrams

Diagram	Contribution to V_R	
tZW	2.01×10^{-5}	
$t\gamma W$	-1.10×10^{-5}	
tHW	0	
tw_0w $+$ tHw	$[(-3.05 \times 10^{-5})$ $+(0.64 \times 10^{-5})$ $+(0.86 \times 10^{-5})]$	$= -1.55 \times 10^{-5}$
tZw	0.10×10^{-5}	
$t\gamma w$	0.69×10^{-5}	
bWZ	$(1.12 + 8.24\,i) \times 10^{-5}$	
$bW\gamma$	$(8.34 - 4.25\,i) \times 10^{-5}$	
bWH	0	
bww_0 $+$ bwH	$[(-0.72 + 3.73\,i \times 10^{-5})$ $+(-0.10 - 2.99\,i \times 10^{-5})$ $+(1.83 - 1.09\,i \times 10^{-5})]$	$= (1.01 - 0.35\,i) \times 10^{-5}$
bwZ	$(0.00 + 0.31\,i) \times 10^{-5}$	
$bw\gamma$	$(-4.47 + 2.29\,i) \times 10^{-5}$	
Ztb	-2.30×10^{-5}	
γtb	-2.78×10^{-5}	
w_0tb $+$ Htb	$[(-0.24 \times 10^{-5})$ $+(0.20 \times 10^{-5})$ $+(-0.99 \times 10^{-5})]$	$= -1.03 \times 10^{-5}$
$\Sigma(EW)$	$(0.06 + 6.23\,i) \times 10^{-5}$	
$gtb(QCD)$	2.68×10^{-3}	
$(QCD + EW)$	$(2.68 + 0.06\,i) \times 10^{-3}$	

3.1 Observables in the W rest frame

Top properties were studied in previous works by means of the observables that we just mentioned. One of the first possibilities are the angular asymmetries for the $t \rightarrow W^+ b$ decay, with the W^+ decaying leptonicaly. The normalized charged lepton angular distribution in the W rest frame can be written as:

$$\frac{1}{\Gamma} \frac{d\Gamma}{d\cos\theta_l} = \frac{3}{8}(1 + \cos\theta_l)^2 F_+ + \frac{3}{8}(1 - \cos\theta_l)^2 F_- + \frac{3}{4}\sin^2\theta_l\, F_0, \tag{5}$$

where $F_0, F_\pm$ are the normalized partial widths of the top decay into the W helicity states, and θ_l is the angle between the charged lepton momentum in the W rest frame and the W momentum in the t rest frame. Then, the asymmetries are defined, in terms of a new parameter z, as follows [10, 21]:

$$A_z = \frac{N(\cos\theta_l > z) - N(\cos\theta_l < z)}{N(\cos\theta_l > z) + N(\cos\theta_l < z)}. \tag{6}$$

5

The z parameter allows to separate the helicity fractions $F_0, F_\pm$. The value $z = 0$ gives the usual forward-backwards asymmetry while $z = \pm(2^{2/3} - 1)$ defines the $A_\mp$ asymmetries, respectively. The first one, A_0 depends only on the $F_\pm$ helicity fractions while $A_\pm$ depends on both F_0 and $F_\pm$.

The helicity fractions, F_0 and $F_\pm$, can be computed in terms of the tbW couplings given in eq. (1), and they can be found, for example, in ref. [22]. Performing the θ_l integration of eq. (6) for a given value of z, the numerator of the asymmetry A_z, in terms of V_L and V_R is:

$$V_L^2 \left(2.48z^3 + 2.00z^2 - 11.45z - 2.00\right) + 0.56zV_LV_R$$
$$+V_R^2 \left(2.48z^3 - 2.00z^2 - 11.45z + 2.00\right). \tag{7}$$

One can now choose the value of the z parameter, within the range $(-1, 1)$, to make zero the leading V_L contribution. In this way we get the maximum sensitivity to V_R. The coefficient of V_L^2 and V_R^2 from eq. (7), are plotted in figure 2. There, it can be seen
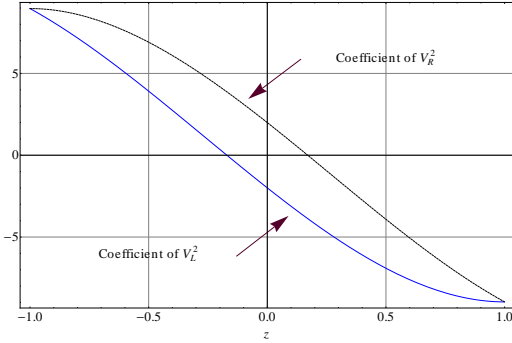

Figure 2: Plot of the coefficients of V_L^2 and V_R^2 from eq. (7) in terms of z.
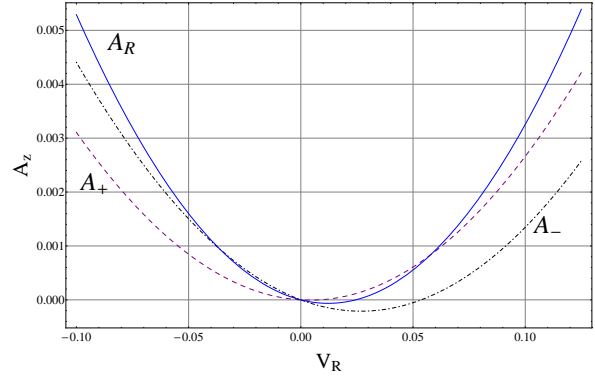
Figure 3: Dependence on the V_R coupling for A_R (blue-solid), eq. (8), and for the usual A_+ (purple-dashed) and A_- (black-dot-dashed) asymmetries, eq. (6).

that for $z = z_R = -0.17$ the coefficient of V_L^2 cancels, leaving the V_R term, in eq. (7), as the leading one. For this z_R the new asymmetry $A_R \equiv A_Z(z = z_R)$ is proportional to V_R and has the form:

$$A_R(V_L, V_R) = \frac{-0.01V_LV_R + 0.48V_R^2}{1.12\left(V_L^2 + V_R^2\right) - 0.07V_LV_R} \simeq -0.01V_R, \tag{8}$$

where the last expression is the value of the asymmetry taking $V_L = 1$ and assuming $|V_R| << 1$. As can be seen this asymmetry is directly proportional to V_R so that a non-zero measurement of it is a direct test of $V_R \neq 0$.

Note that the leading contribution to the usual $A_\pm$ asymmetries comes from V_L^2 so that in order to be sensitive to V_R one needs to subtract this SM central value. In figure 3 we show the V_R dependence of A_R and also, for comparison, the dependence of $A_\pm$, with the V_L^2 leading contribution subtracted. As can be seen there A_R may allow more precise bounds on V_R. Besides, it is directly proportional to V_R and eliminates other uncertainties that the V_L dependence in $A_\pm$ may introduce.

For polarized top it is possible to define asymmetries with respect to the normal and transverse spin directions. These were studied in ref. [11], but they are not sensitive to the V_R coupling so we are not going to consider them in our analysis.

3.2   Observables in the top rest frame

Angular distribution of the decay products for the weak process $t \to W^+ b$ carries information about the spin of the decaying top. Then, angular asymmetries can be built to test the Lorentz structure of the vertex. We will follow the same procedures described previously, in order to optimize the sensitivity of the observables to V_R but, in this case, for the asymmetries in the top rest frame.

For the top decay $t \to W^+ b \to l^+ \nu b, q \bar{q}' b$, the angular distribution of the product $X = l^+, \nu, q, \bar{q}', W^+, b$, in the top rest frame, is given by:

$$\frac{1}{\Gamma} \frac{d\Gamma}{d\cos\theta_X} = \frac{1}{2} \left(1 + \alpha_X \cos\theta_X \right), \tag{9}$$

where θ_X is the angle between the momentum of X and the top spin direction, and α_X are the spin-analyzer powers, given in references [11,22–24,29] in terms of the couplings shown in eq. (1). Then, an asymmetry can be defined as:

$$A_X^z \equiv \frac{N(\cos\theta_X > z) - N(\cos\theta_X < z)}{N(\cos\theta_X > z) + N(\cos\theta_X < z)} = \frac{1}{2} \left[\alpha_X (1 - z^2) - 2z \right]. \tag{10}$$

For $z = 0$, one gets the usual forward-backward asymmetry:

$$A_X \equiv \frac{N(\cos\theta_X > 0) - N(\cos\theta_X < 0)}{N(\cos\theta_X > 0) + N(\cos\theta_X < 0)} = \frac{\alpha_X}{2}. \tag{11}$$

Sensitivity to V_R and V_L for this asymmetry have already been given for $X = l^+, b, \nu$ in the t-channel single top production in refs. [11,30]. In order to define a new asymmetry directly proportional to the V_R coupling one can again extract the SM leading contribution, given by the V_L^2 term in the A_X^z asymmetry, and make it zero. For the $X = l, \nu, b$ cases, the eq. (10) is:

$$
\begin{aligned}
A_l^z &= \frac{-1}{2 \left(V_L^2 + V_R^2 - 0.06 V_L V_R \right)} \times \\
&\quad \left[V_L^2 \left(-\frac{1}{2} z^2 - z + \frac{1}{2} \right) + V_R^2 \left(-0.16 z^2 - z + 0.16 \right) \right. \\
&\quad \left. + 0.06 V_L V_R \left(\frac{1}{2} z^2 + z - \frac{1}{2} \right) \right],
\end{aligned} \tag{12}
$$

$$
\begin{aligned}
A_b^z &= \frac{0.20}{V_L^2 + V_R^2 - 0.06 V_L V_R} \times \left[V_L^2 \left(z^2 - 4.93 z - 1 \right) \right. \\
&\quad \left. + V_R^2 \left(-z^2 - 4.93 z + 1 \right) + 0.31 z V_L V_R \right],
\end{aligned} \tag{13}
$$

$$A_\nu^z = \frac{0.16}{V_L^2 + V_R^2 - 0.06 V_L V_R} \times \left[V_L^2 \left(z^2 - 6.30z - 1 \right) \right.$$
$$+ V_R^2 \left(3.15 z^2 - 6.30 z - 3.15 \right)$$
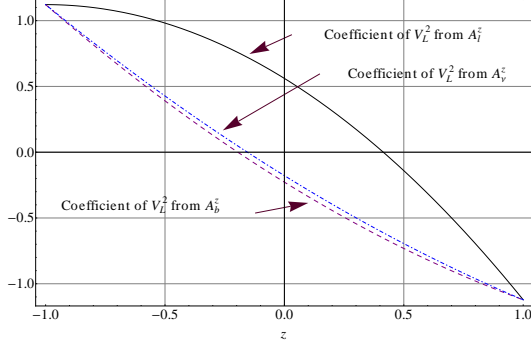$$\left. + V_L V_R \left(-0.19 z^2 + 0.39 z + 0.19 \right) \right]. \tag{14}$$

Figure 4: Plot of the coefficients of V_L^2, in terms of z, from eqs. (12), (13) and (14).
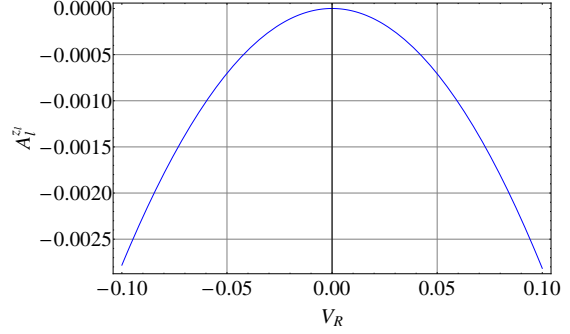
Figure 5: Dependence on the V_R coupling for the A_l^{zl} asymmetry, eq. (16).

Figure 4 shows the behavior of the V_L^2 coefficient from the A_l, A_b and A_ν asymmetries. We can choose z in order to make the leading coefficients of eqs. (12), (13) and (14) to be zero. These z values are:

$$z_l = \sqrt{2} - 1, \quad z_b = -0.20, \quad z_\nu = -0.16, \tag{15}$$

and then, the new asymmetries are:

$$A_l^{zl} = \frac{-0.28 V_R^2}{V_L^2 + V_R^2 - 0.06 V_L V_R} \simeq -0.28 V_R^2, \tag{16}$$

$$A_b^{zb} = \frac{0.39 V_R^2 - 0.01 V_L V_R}{V_L^2 + V_R^2 - 0.06 V_L V_R} \simeq -0.01 V_R, \tag{17}$$

$$A_\nu^{z\nu} = \frac{0.02 V_L V_R - 0.33 V_R^2}{V_L^2 + V_R^2 - 0.06 V_L V_R} \simeq 0.02 V_R, \tag{18}$$

where in the last expression we show the value of the asymmetries for $V_L = 1$ and assuming $|V_R| << 1$. From eq. (12) one can see that unfortunately, for the A_l asymmetry, the same value of z that cancels the coefficient of V_L^2 also cancels the $V_L V_R$ term, in such a way that a poorer sensitivity to the coupling will be expected from this observable because the surviving term is V_R^2 instead of $V_L V_R$.

In figures 5, 6 and 7 we show the dependence on V_R for the new A_l^{zl}, A_b^{zb} and $A_\nu^{z\nu}$ observables. We have explicitly checked that the usual forward-backward asymmetries for the same decay product have a very similar behavior as the ones shown in the figures, once the leading V_L^2 contribution is removed. However, the new observables again have the advantage that are proportional to V_R so that their measurement may provide a direct bound or measurement of the V_R coupling with no assumption on the value of the V_L^2 leading term.
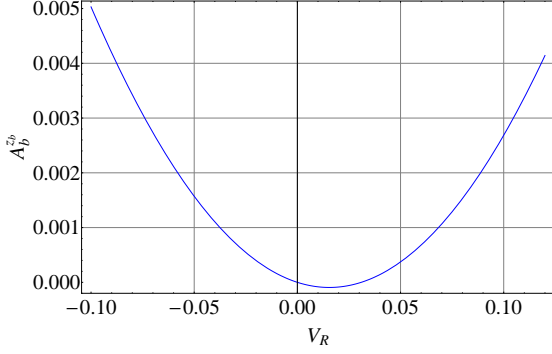
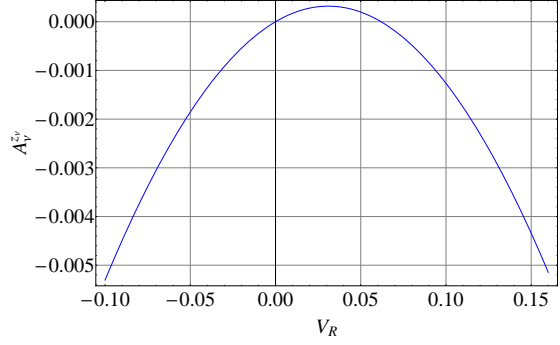Figure 6: Dependence on the V_R coupling for the $A_b^{z_b}$ asymmetry, eq. (17)

Figure 7: Dependence on the V_R coupling for the $A_\nu^{z_\nu}$ asymmetry, eq. (18).

3.3 Spin correlations in $t\bar{t}$ production

The top–antitop spin correlations depend on the Lorentz structure of the tbW vertex. This structure can be studied through the measurement of the angular distributions of the decay products for the $t \to W^+ b$ and $\bar{t} \to W^- \bar{b}$ processes, that carry information on the top and antitop spin correlation terms. In particular, using the notation of previous section, the double angular distribution – of the decay products X, from top, and $\bar{X}'$, from antitop – can be written as [25, 26]:

$$\frac{1}{\sigma}\frac{d\sigma}{d\cos\theta_X \, d\cos\theta_{\bar{X}'}} = \frac{1}{4}\left(1 + C\,\alpha_X\,\alpha_{\bar{X}'}\,\cos\theta_X\,\cos\theta_{\bar{X}'}\right),\tag{19}$$

where θ_X ($\theta_{\bar{X}'}$) is the angle between the momentum of the decay product X ($\bar{X}'$) and the momentum of the top (antitop) quark in the $t\bar{t}$ center-of-mass frame, α_X and $\alpha_{\bar{X}'}$ are the spin analyzer powers of particles X and $\bar{X}'$, respectively. C is a coefficient that weights the spin correlation between the quark and the antiquark. Then, one can define the asymmetry

$$
\begin{aligned}
A_{X\bar{X}'}^{z_1 z_2} &\equiv \frac{1}{\sigma}\Bigg[\int_{z_1}^{1} d(\cos\theta_X) \int_{z_2}^{1} d(\cos\theta_{\bar{X}'}) \frac{d\sigma}{d\cos\theta_X \, d\cos\theta_{\bar{X}'}} \\
&+ \int_{-1}^{z_1} d(\cos\theta_X) \int_{-1}^{z_2} d(\cos\theta_{\bar{X}'}) \frac{d\sigma}{d\cos\theta_X \, d\cos\theta_{\bar{X}'}} \\
&- \int_{-1}^{z_1} d(\cos\theta_X) \int_{z_2}^{1} d(\cos\theta_{\bar{X}'}) \frac{d\sigma}{d\cos\theta_X \, d\cos\theta_{\bar{X}'}} \\
&- \int_{z_1}^{1} d(\cos\theta_X) \int_{-1}^{z_2} d(\cos\theta_{\bar{X}'}) \frac{d\sigma}{d\cos\theta_X \, d\cos\theta_{\bar{X}'}} \Bigg].
\end{aligned}
\tag{20}
$$

The different regions of integration for this asymmetry are plotted in figure 8. There, the number of events on each of the regions is collected and the sign of their contribution to the asymmetry is also indicated. The particular case $z_1 = z_2 = 0$ corresponds to the usual spin correlation asymmetry:

$$A_{X\bar{X}'} = \frac{N\left(\cos\theta_X\,\cos\theta_{\bar{X}'} > 0\right) - N\left(\cos\theta_X\,\cos\theta_{\bar{X}'} < 0\right)}{N\left(\cos\theta_X\,\cos\theta_{\bar{X}'} > 0\right) + N\left(\cos\theta_X\,\cos\theta_{\bar{X}'} < 0\right)}.\tag{21}$$
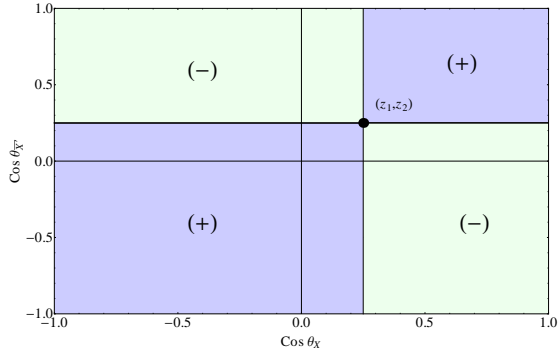
9

Figure 8: Regions of integration and sign of the contribution to the spin correlation asymmetry $A_{X\bar{X}'}^{z_1 z_2}$ defined in eq. (20), depending on the point (z_1, z_2)
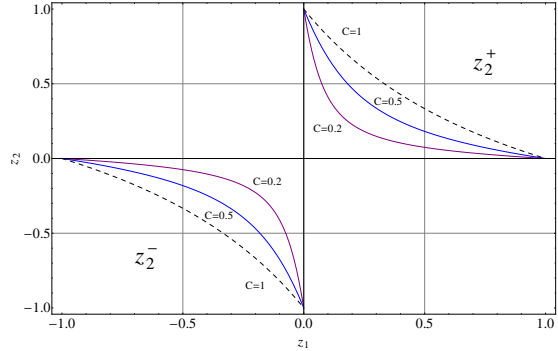
Figure 9: Values of z_1 and z_2 that makes zero the V_L leading terms of the $A_{ll'}^{z_1 z_2}$ asymmetry, eq. (22), for different values of the spin correlation coefficient C.

For the $A_{X\bar{X}'}^{z_1 z_2}$ asymmetry, eq. (20), there is a range of values of z_1 and z_2 that cancel the leading V_L^4 contribution, in such a way that the observable becomes proportional to the V_R coupling. For the $X = l$, $\bar{X}' = l'$ case, these values satisfy the relation:

$$z_2^\pm = \frac{-2z_1 \pm \sqrt{C^2(1-z_1^2)^2 + 4z_1^2}}{C(1-z_1^2)}. \tag{22}$$

Similarly to what happened for A_l^z, in eq. (12), for values of z_1 and z_2 satisfying the previous equation, the coefficient of $V_L^3 V_R$ in the asymmetry also accidentally cancels. Then, it remains the V_R^2 coupling as the leading contribution. Solutions to eq. (22) are plotted in figure 9 where it can be seen that the values of z_1 and z_2 are restricted to be in the first quadrant (for the z_2^+ solution) or in the third one (for the z_1^- solution). In addition to the trivial solutions of eq. (22), i.e. $z_1 = \pm 1, z_2 = 0$, that reproduces the usual $A_{ll'}$ asymmetry, one can improve the computation by finding the values of z_1 and z_2 that, satisfying eq. (22), also maximize the coefficient of the leading V_R^2 term in eq.(20), namely:

$$2.00\, V_R^2 \left[z_1 z_2 + 0.08\, C \left(z_1^2 \left(1 - z_2^2\right) + z_2^2 - 1 \right) \right]. \tag{23}$$

This can be trivially done and the result is

$$z_1 = z_2 = z_{ll'} \equiv \pm\sqrt{1 + \frac{2}{C} - \frac{2}{C}\sqrt{1 + C}}, \tag{24}$$

that correspond to the intersection of the curves of figure 9 with the diagonal line of the first and third quadrants. These values of z_1, z_2 give a maximum sensitivity of the $A_{ll'}^{z_1 z_2}$ asymmetry to the V_R coupling.

In figure 10 we show the dependence on the V_R coupling for the $A_{ll'}^{z_1 z_2}$ asymmetry in eq. (20), for $C = 0.4$ [11] , and $z_1 = z_2 = z_{ll'} = 0.29$, given by eq. (24).

The same procedure followed here can be used for other decay products of the $W^\pm$. For $t\bar{t} \to l\,\nu\,b\,\bar{\nu}\,l'\,\bar{b}$ final state, the values of z_1 and z_2 that cancels the coefficient of
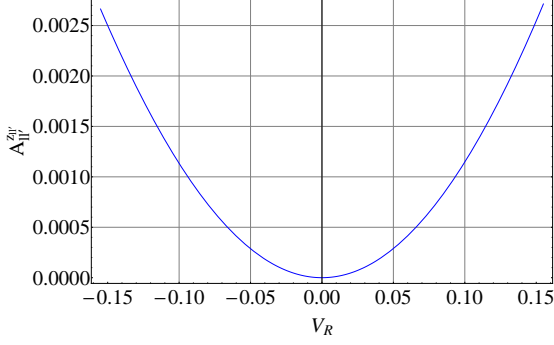
10

Figure 10: Dependence on V_R coupling for $A_{ll'}^{z_1 z_2}$ in eq. (20), for $C = 0.4$ and $z_1 = z_2 = z_{ll'} = 0.29$.
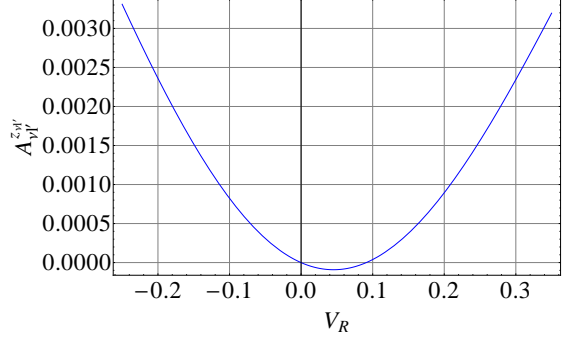
Figure 11: Dependence on the V_R coupling for $A_{\nu l'}^{z_1 z_2}$, eq. (20), for $C = 0.4$ and $z_1 = -z_2 = z_{\nu l'} = 0.17$.

the leading V_L^4 term in the $A_{\nu l'}^{z_1 z_2}$ asymmetry ($X = \nu$, $\bar{X}' = l'$ in eq. (20)), satisfy a quadratic equation

$$z_1 z_2 = -\beta(1 - z_1^2)(1 - z_2^2), \quad \beta = 0.08C, \tag{25}$$

and the solution is

$$z_2^{\pm} = \frac{1}{2\beta(1 - z_1^2)} \left[z_1 \pm \sqrt{z_1 + 4\beta^2(1 - z_1)^2} \right]. \tag{26}$$

Here, $-1 \leq z_1 \leq 0$ for the z_2^+ solution and $0 \leq z_1 \leq 1$ for the z_2^- solution of eq. (26), in order to satisfy $|z_2^{\pm}| < 1$. In that case, these set of $z_{1,2}$ values do not cancel the V_R term of the asymmetry, that remains as the leading one:

$$-0.12 \left[z_1 z_2 - \frac{C}{4}(1 - z_1^2)(1 - z_2^2) \right] V_R. \tag{27}$$

One can easily find the values that maximize this coefficient and simultaneously verify eq. (26):

$$z_1 = -z_2 = z_{\nu l'} \equiv \pm \sqrt{1 + \frac{1}{2\beta} - \frac{1}{2\beta}\sqrt{1 + 2\beta}} \tag{28}$$

In figure 11 we show the dependence of the spin correlation asymmetry $A_{\nu l'}^{z_{\nu l'} z_{\nu l'}}$ on V_R, for z_1, z_2 given by eq. (28) with $C = 0.4$. Note that the sensitivity of both asymmetries shown in figures 10 and 11 is rather similar.

Another spin correlation considered in the literature is the angular distribution of the top (antitop) decay products defined as [31]:

$$\frac{1}{\sigma}\frac{d\sigma}{d\cos\varphi_{X\bar{X}'}} = \frac{1}{4}\left(1 + D\,\alpha_X\,\alpha_{\bar{X}'}\cos\varphi_{X\bar{X}'}\right), \tag{29}$$

where $\varphi_{X\bar{X}'}$ is the angle between the momentum of the X particle in the t rest frame, and that of the X' one, in the $\bar{t}$ rest frame. D is the spin correlation coefficient. Then, one can construct the following asymmetry:

$$\tilde{A}_{X\bar{X}'}^z \equiv \frac{N(\cos\varphi_{X\bar{X}'} > z) - N(\cos\varphi_{X\bar{X}'} < z)}{N(\cos\varphi_{X\bar{X}'} > z) + N(\cos\varphi_{X\bar{X}'} < z)} = \frac{1}{2}\left(\alpha_X\,\alpha_{\bar{X}'}(1 - z^2) - 2z\right). \tag{30}$$

11

For $z = 0$ one gets the usual forward-backward spin correlation asymmetry

$$\tilde{A}_{X\bar{X}'} = \frac{1}{2} D \, \alpha_X \, \alpha_{\bar{X}'}. \tag{31}$$

For both $W^{\pm}$ leptonic decays, $X = l$ and $\bar{X}' = l'$, and following similar procedures as in the previous sections, we can find the value of z that cancels the V_L^4 leading term in eq. (30):

$$z = \tilde{z}_{ll'} \equiv \frac{1}{D} \left(1 - \sqrt{1 + D^2} \right). \tag{32}$$

This value also cancels the V_R term so that the V_R^2 contribution is the dominant one. Then, for $D = -0.29$ [11], the $\tilde{A}_{ll'}^z$ asymmetry is:

$$\tilde{A}_{ll'}^{\tilde{z}_{ll'}} = \frac{-0.19 V_L^2 V_R^2 + 0.01 V_L V_R^3 - 0.13 V_R^4}{(V_L^2 - 0.06 V_L V_R + V_R^2)^2} \simeq -0.19 V_R^2 \tag{33}$$

where again, in the last term, we show the asymmetry for $V_L = 1$ and $|V_R| << 1$. This asymmetry can be seen in figure 12.
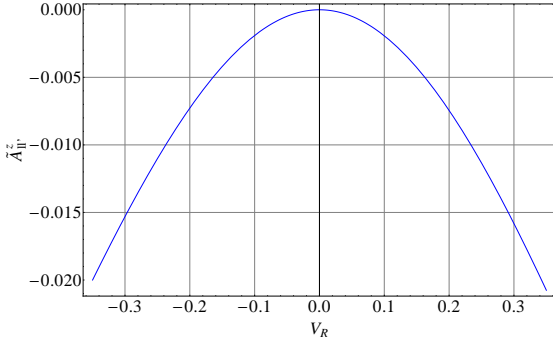

Figure 12: Dependence on the V_R coupling for the $\tilde{A}_{ll'}^z$ asymmetry, eq. (33), for $D = -0.29$ and $z = \tilde{z}_{ll'}$ given by eq. (32).
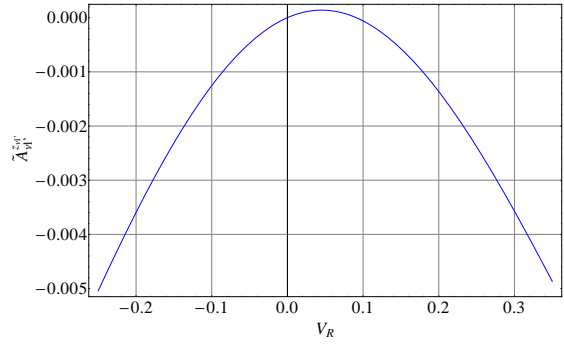
Figure 13: Dependence on the V_R coupling for the $\tilde{A}_{\nu l'}^z$ asymmetry, eq. (35), for $D = -0.29$ and $z = z = \tilde{z}_{\nu l'}$ given by eq. (34).

Analogously, for W leptonic decays with neutrino-lepton final state, $X = \nu$, $\bar{X}' = l'$, the z-value that cancels the V_L^4 term in eq. (30) is

$$z = \tilde{z}_{\nu l'} = -\frac{3.15}{D} \left(1 - \sqrt{1 + \left(\frac{D}{3.15} \right)^2} \right), \tag{34}$$

and then, the $\tilde{A}_{\nu l'}^z$ asymmetry, for $D = -0.29$, is:

$$\tilde{A}_{\nu l'}^{\tilde{z}_{\nu l'}} = \frac{0.006 V_L^3 V_R - 0.068 V_L^2 V_R^2 + 0.006 V_L V_R^3}{(V_L^2 - 0.062 V_L V_R + V_R^2)^2} \simeq 0.006 V_R. \tag{35}$$

The last term in this equation is given for $V_L = 1$ and $|V_R| << 1$. This asymmetry is depicted in figure 13. Note that in this case the sensitivity to V_R is lower than the one obtained in some of the previous observables due to the small coefficients in the numerator of eq. (35).

We checked that the expressions of the observables defined for the V_R coupling in this section show a behavior comparable to the one obtained from the expressions of the observables defined in the literature, once the V_L leading contribution is removed. Moreover, the observables defined here have the advantage of being directly proportional to the V_R term that we want to test.

4   Conclusions

We computed the SM one-loop QCD and electroweak contribution to V_R. Due to accidental cancellations between the diagrams, the leading contribution is mainly coming from QCD, it is real and of the order of 10^{-3}. Any measurement of observables that may lead to V_R above to 10^{-3} should be interpreted as new physics effects.

We also have proposed new observables that may provide a direct measurement of the right coupling. We found that for several angular asymmetries considered in the literature it is possible to define new observables, with an optimal choice of parameters, in such a way that they become a direct probe of V_R. These observables include angular asymmetries in the W rest frame, angular asymmetries in the top rest frame and also spin correlations. All the new observables defined in this paper are proportional to V_R and then suitable for a direct determination of this coupling. In some cases the behavior shown by the expressions for our observables, presents a better sensitivity to V_R (like it is shown in Figure 3). While the asymmetries usually considered in the literature have leading contributions from V_L, the new asymmetries that we have studied here have as a leading term the V_R right coupling we are interested in. These asymmetries can be measured with LHC data, where a huge number of top events are being collected, in order to obtain a direct measurement on the standard model contribution to the right top quark.

5   Acknowledgments

Appendix A Diagram contributions

Using the following definitions for the denominators:

$$A_Z = x^2 \left[\left((y-1)r_b^2 + 1 \right) y - r_w^2(y-1) \right] - r_z^2(x-1), \tag{36}$$

$$B_Z = x \left\{ \left[(x(y-1)+1) \, r_b^2 + x - 1 \right] y - r_z^2(y-1) \right\} - r_w^2(x-1) \left[x(y-1)+1 \right], \tag{37}$$

$$C_Z = (x-1)(xy-1)r_b^2 - r_w^2(x-1)x(y-1) + r_z^2 xy + x(y-1)(xy-1), \tag{38}$$

$$\{A_\gamma, B_\gamma, C_\gamma\} = \{A_Z, B_Z, C_Z\} \, (r_z \to 0), \tag{39}$$

$$\{A_H, B_H, C_H\} = \{A_Z, B_Z, C_Z\} \, (r_z \to r_h). \tag{40}$$

with

$$r_x \equiv \frac{m_x}{m_t} \tag{41}$$

and taking the usual definition for the SM couplings

$$a_t = -a_b = 1, \quad v_b = -1 + \frac{4s_w^2}{3} \quad \text{and} \quad v_t = 1 - \frac{8s_w^2}{3}, \tag{42}$$

the expression for the contribution of each diagram is given by:

$$I^{tZW} = -\frac{1}{32\pi s_w^2} \times \int_0^1 dx \int_0^1 dy \, \frac{2x^2 y \left[v_t(1+2xy) - a_t(5-2xy) \right]}{A_Z}, \tag{43}$$

$$I^{t\gamma W} = -\frac{1}{8\pi} Q_t \times \int_0^1 dx \int_0^1 dy \, \frac{2x^2 y(1+2xy)}{A_\gamma}, \tag{44}$$

$$I^{tHW} = 0, \tag{45}$$

$$I^{tw0w} + I^{tHw} = \frac{1}{16\pi s_w^2} \frac{1}{r_w^2} \times \int_0^1 dx \int_0^1 dy \left\{ -\frac{x^3 y \left[1 + y - r_b^2(1-y) \right]}{A_Z} \right.$$
$$\left. + (1-rb^2) \frac{x^3 y(1-y)}{A_H} + x \log \frac{A_H}{A_Z} \right\}, \tag{46}$$

$$I^{tZw} = \frac{1}{32\pi c_w^2} \times \int_0^1 dx \int_0^1 dy \, \frac{2x^2 y(a_t - v_t)}{A_Z}, \tag{47}$$

$$I^{t\gamma w} = -\frac{1}{8\pi} Q_t \times \int_0^1 dx \int_0^1 dy \, \frac{2x^2 y}{A_\gamma}, \tag{48}$$

$$I^{bWZ} = \frac{1}{32\pi s_w^2} \times \int_0^1 dx \int_0^1 dy \, \frac{2x^2 y \left[v_b(1+2xy) - a_b(5-2xy) \right]}{B_Z}, \tag{49}$$

$$I^{bW\gamma} = \frac{1}{8\pi} Q_b \times \int_0^1 dx \int_0^1 dy \, \frac{2x^2 y(1+2xy)}{B_\gamma}, \tag{50}$$

$$I^{bWH} = 0, \tag{51}$$

$$
\begin{aligned}
I^{bww_0} + I^{bwH} \;=\; & \frac{1}{16\pi s_w^2}\frac{1}{r_w^2} \times \int_0^1 dx \int_0^1 dy \left\{ \frac{x^2 y\left[1 - x - r_b^2\left(1 - x(1-2y)\right)\right]}{B_Z} \right. \\
& \left. -(1 - r_b^2)\frac{x^2 y(1-x)}{B_H} + x \log \frac{B_H}{B_Z} \right\},
\end{aligned}
\tag{52}
$$

$$I^{bwZ} = \frac{1}{32\pi c_w^2} \times \int_0^1 dx \int_0^1 dy\, \frac{2x^2 y (v_b - a_b)}{B_Z}, \tag{53}$$

$$I^{bw\gamma} = -\frac{1}{8\pi}\,Q_b \times \int_0^1 dx \int_0^1 dy\, \frac{2x^2 y}{B_\gamma}, \tag{54}$$

$$
\begin{aligned}
I^{Ztb} \;=\; & \frac{1}{32\pi c_w^2 s_w^2} \\
& \times \int_0^1 dx \int_0^1 dy\, \frac{x\left[a_b(1+xy) - v_b(1-xy)\right]\left[a_t(1+xy) - v_t(1-xy)\right]}{C_Z},
\end{aligned}
\tag{55}
$$

$$I^{\gamma tb} = \frac{1}{2\pi}\,Q_b\,Q_t \times \int_0^1 dx \int_0^1 dy\, \frac{x(1-xy)^2}{C_\gamma}, \tag{56}$$

$$
\begin{aligned}
I^{w_0 tb} + I^{Htb} \;=\; & \frac{1}{16\pi s_w^2} \times \\
& \int_0^1 dx \int_0^1 dy\, x^2(1-x)(1-y)\left\{ \frac{-1}{C_Z} + \frac{1}{C_H} + \frac{x}{r_w^2}\log\frac{C_Z}{C_H} \right\}.
\end{aligned}
\tag{57}
$$

Appendix B   Contribution of diagrams with a photon

$$
\begin{aligned}
I_0^{t\gamma W} = \frac{-2}{r_b}\left\{ 1 + \left[\frac{(1 - r_w^2 - r_b^2 - \Delta)(1 - r_w^2 - 3r_b^2 - \Delta)}{4r_b^2\,\Delta} \log\left(\frac{r_w^2}{1 - r_w^2} \right) \right] \right. \\
\left. + \left[\Delta \to -\Delta \right] \right\},
\end{aligned}
\tag{58}
$$

$$
I_0^{t\gamma w} = \left[\frac{-1}{r_b\,\Delta}(1 - r_b^2 - r_w^2 - \Delta) \log\left(\frac{1 + r_w^2 - r_b^2 + \Delta}{2r_w} \right) \right] + \left[\Delta \to -\Delta \right],
\tag{59}
$$

15

$$I_0^{bW\gamma} = \frac{2}{r_b} + \left\{ \frac{-2\left(1 - r_b^2 - r_w^2 + \Delta\right)}{r_b \Delta (1 + r_b^2 - r_w^2 + \Delta)^2} \left[(1 - r_w^2)^2 - r_b^2(1 + r_w^2) + \Delta(1 - r_w^2) \right. \right.$$

$$\left. \left. - 2r_b^2(1 - r_w^2 + \Delta) \log\left(\frac{2r_b^2}{1 - r_w^2 - r_b^2 + \Delta} \right) \right] \right\} + \left\{ \Delta \to -\Delta \right\}$$

$$+ \left[4\pi\, i\, r_b\, \frac{(1 - r_w^2 - r_b^2 + \Delta)(1 - r_w^2 + \Delta)}{(1 - r_w^2 + r_b^2 + \Delta)^2 \Delta} \right] - \left[\Delta \to -\Delta \right], \tag{60}$$

$$I_0^{bw\gamma} = -2\, r_b \left\{ \left(\pi\, i\, \frac{1 - r_b^2 - r_w^2 + \Delta}{\Delta(1 + r_b^2 - r_w^2 + \Delta)} \right) - \left(\Delta \to -\Delta \right) \right.$$

$$\left. + \left[\frac{1 - r_b^2 - r_w^2 + \Delta}{\Delta(1 + r_b^2 - r_w^2 + \Delta)} \log\left(\frac{2r_b^2}{1 - r_b^2 - r_w^2 + \Delta} \right) \right] + \left[\Delta \to -\Delta \right] \right\}, \tag{61}$$

$$I_0^{\gamma tb} = \frac{2\, r_b}{\Delta} \log\left(\frac{1 - r_w^2 + r_b^2 + \Delta}{1 - r_w^2 + r_b^2 - \Delta} \right), \tag{62}$$

with

$$\Delta = \sqrt{(1 - r_w^2)^2 + r_b^4 - 2r_b^2(1 - r_w^2)}.$$

In the limit $r_b \to 0$, the formulas get a simplest expression:

$$I_0^{t\gamma W} \xrightarrow{r_b \to 0} -\frac{r_b}{(1 - r_w^2)^3} \left[(3 - 8r_w^2 + 5r_w^4) + 4r_w^2(1 - 2r_w^2)\log(r_w) \right], \tag{63}$$

$$I_0^{t\gamma w} \xrightarrow{r_b \to 0} \frac{2\, r_b}{(1 - r_w^2)^2} \left[1 - r_w^2 + r_w^2 \log(r_w^2) \right], \tag{64}$$

$$I_0^{bW\gamma} \xrightarrow{r_b \to 0} 2\, r_b \left[\pi i\, \frac{(2 + r_w^2 + r_w^4)}{1 - r_w^2} + \frac{2\, r_w^2 \left(1 - 2r_w^2 + 2r_w^6 - r_w^8\right)}{(1 - r_w^2)^4} \log(r_w) \right.$$

$$\left. + 1 - \frac{2 - r_w^2(5 - 4r_w^2 + 2r_w^2 - 2r_w + r_w^8)}{(1 - r_w^2)^4} \log(1 - r_w^2) \right], \tag{65}$$

$$I_0^{bw\gamma} \xrightarrow{r_b \to 0} \frac{-r_b}{1 - r_w^2} \left[2\pi\, i\, (1 + r_w^2) + \log\left(\frac{r_b^2}{1 - r_w^2} \right) + r_w^2 \log\left(\frac{r_w^2}{1 - r_w^2} \right) \right], \tag{66}$$

$$I_0^{\gamma tb} \xrightarrow{r_b \to 0} -\frac{4\, r_b}{1 - r_w^2} \log\left(\frac{r_b}{1 - r_w^2} \right), \tag{67}$$

References

[1] F.-P. Schilling, *Top Quark Physics at the LHC: A Review of the First Two Years, Int. J. Mod. Phys.* **A27** (2012) 1230016, [`arXiv:1206.4484`].

[2] R. Hawkings, *Top quark physics at the LHC, Comptes Rendus Physique* **16** (2015) 424–434.

[3] W. Bernreuther, *Top quark physics at the LHC, J. Phys. G* **35** (2008) 083001, [`arXiv:0805.1333`].

[4] **CDF Collaboration** Collaboration, F. Abe et al., *Observation of top quark production in $\bar{p}p$ collisions, Phys. Rev. Lett.* **74** (1995) 2626–2631, [`hep-ex/9503002`].

[5] **D0 Collaboration** Collaboration, S. Abachi et al., *Observation of the top quark, Phys. Rev. Lett.* **74** (1995) 2632–2637, [`hep-ex/9503003`].

[6] C. Deterre, *W helicity and constraints on the Wtb vertex at the Tevatron, Nuovo Cim.* **C035N3** (2012) 125–129, [`arXiv:1203.6802`].

[7] **D0 Collaboration** Collaboration, V. M. Abazov et al., *Search for anomalous Wtb couplings in single top quark production in $p\bar{p}$ collisions at $\sqrt{s} = 1.96$ TeV, Phys. Lett. B* **708** (2012) 21–26, [`arXiv:1110.4592`].

[8] **D0** Collaboration, V. M. Abazov et al., *Search for anomalous Wtb couplings in single top quark production, Phys. Rev. Lett.* **101** (2008) 221801, [`arXiv:0807.1692`].

[9] C. Bernardo, N. F. Castro, M. C. N. Fiolhais, H. Gonçalves, A. G. C. Guerra, M. Oliveira, and A. Onofre, *Studying the Wtb vertex structure using recent LHC results, Phys. Rev.* **D90** (2014), no. 11 113007, [`arXiv:1408.7063`].

[10] F. del Aguila and J. Aguilar-Saavedra, *Precise determination of the Wtb couplings at CERN LHC, Phys.Rev.* **D67** (2003) 014009, [`hep-ph/0208171`].

[11] J. Aguilar-Saavedra and J. Bernabéu, *W polarisation beyond helicity fractions in top quark decays, Nucl. Phys. B* **840** (2010) 349–378, [`arXiv:1005.5382`].

[12] J. Drobnak, S. Fajfer, and J. F. Kamenik, *New physics in $t->bW$ decay at next-to-leading order in QCD, Phys. Rev.* **D82** (2010) 114008, [`arXiv:1010.2402`].

[13] S. D. Rindani and P. Sharma, *Probing anomalous tbW couplings in single-top production using top polarization at the Large Hadron Collider, JHEP* **1111** (2011) 082, [`arXiv:1107.2597`].

[14] Q.-H. Cao, B. Yan, J.-H. Yu, and C. Zhang, *A General Analysis of Wtb anomalous Couplings,* `arXiv:1504.0378`.

[15] A. V. Prasath, R. M. Godbole, and S. D. Rindani, *Longitudinal top polarisation measurement and anomalous Wtb coupling*, Eur. Phys. J. **C75** (2015), no. 9 402, [`arXiv:1405.1264`].

[16] **Particle Data Group** Collaboration, K. Olive et al., *Review of Particle Physics*, Chin.Phys. **C38** (2014) 090001.

[17] M. Moreno Llácer, *Search for CP violation in single top quark events with the ATLAS detector at LHC*. PhD thesis, Valencia U., IFIC, 2014.

[18] G. A. González-Sprinberg, R. Martinez, and J. Vidal, *Top quark tensor couplings*, JHEP **07** (2011) 094, [`arXiv:1105.5601`]. [Erratum: JHEP05,117(2013)].

[19] L. Duarte, G. A. González-Sprinberg, and J. Vidal, *Top quark anomalous tensor couplings in the two-Higgs-doublet models*, JHEP **1311** (2013) 114, [`arXiv:1308.3652`].

[20] W. Bernreuther, P. Gonzalez, and M. Wiebusch, *The Top Quark Decay Vertex in Standard Model Extensions*, Eur. Phys. J. C **60** (2009) 197–211, [`arXiv:0812.1643`].

[21] B. Lampe, *Forward - backward asymmetry in top quark semileptonic decay*, Nucl.Phys. **B454** (1995) 506–526.

[22] J. Aguilar-Saavedra, J. Carvalho, N. F. Castro, F. Veloso, and A. Onofre, *Probing anomalous Wtb couplings in top pair decays*, Eur.Phys.J. **C50** (2007) 519–533, [`hep-ph/0605190`].

[23] B. Grzadkowski and Z. Hioki, *New hints for testing anomalous top quark interactions at future linear colliders*, Phys.Lett. **B476** (2000) 87–94, [`hep-ph/9911505`].

[24] R. M. Godbole, S. D. Rindani, and R. K. Singh, *Lepton distribution as a probe of new physics in production and decay of the t quark and its polarization*, JHEP **0612** (2006) 021, [`hep-ph/0605100`].

[25] T. Stelzer and S. Willenbrock, *Spin correlation in top quark production at hadron colliders*, Phys.Lett. **B374** (1996) 169–172, [`hep-ph/9512292`].

[26] G. Mahlon and S. J. Parke, *Angular correlations in top quark pair production and decay at hadron colliders*, Phys.Rev. **D53** (1996) 4886–4896, [`hep-ph/9512264`].

[27] J. Bernabéu, G. González-Sprinberg, and J. Vidal, *Normal and transverse single tau polarization at the Z peak*, Phys. Lett. B **326** (1994) 168–174.

[28] J. Bernabeu, G. González-Sprinberg, M. Tung, and J. Vidal, *The Tau weak magnetic dipole moment*, Nucl.Phys. **B436** (1995) 474–486, [`hep-ph/9411289`].

[29] B. Grzadkowski and Z. Hioki, *Decoupling of anomalous top decay vertices in angular distribution of secondary particles*, *Phys.Lett.* **B557** (2003) 55–59, [hep-ph/0208079].

[30] J. Aguilar-Saavedra, J. Carvalho, N. Castro, M. Fiolhais, A. Onofre, et al., *Study of ATLAS sensitivity to asymmetries in single top events*, *Nuovo Cim.* **B123** (2008) 1323–1324.

[31] W. Bernreuther, A. Brandenburg, Z. Si, and P. Uwer, *Top quark pair production and decay at hadron colliders*, *Nucl.Phys.* **B690** (2004) 81–137, [hep-ph/0403035].